DMD Fast Forward. Published on January 8, 2013 as doi:10.1124/dmd.112.050344
This article has not been copyedited and formatted. The final version may differ from this version.

Drug transporters on arachnoid barrier cells contribute to the blood-cerebrospinal fluid barrier

Kazuto Yasuda, Cynthia Cline, Peter Vogel, Mihaela Onciu, Soghra Fatima, Brian P. Sorrentino, Ranjit K. Thirumaran, Sean Ekins, Yoshihiro Urade, Ko Fujimori and Erin G. Schuetz

Department of Pharmaceutical Sciences, St. Jude Children's Research Hospital, Memphis, Tennessee (K.Y., C.C., R.K.T., E.G.S.).

Department of Pathology, St. Jude Children's Research Hospital, Memphis, Tennessee (P.V., M.O.). Department of Hematology, St. Jude Children's Research Hospital, Memphis, Tennessee (S.F., B.P.S.).

Collaborations in Chemistry, Fuquay-Varina, North Carolina (S.E.).

Dept of Molecular Behavioral Biology, Osaka Bioscience Institute, Osaka, Japan (Y.U.).

Laboratory of Biodefense and Regulation, Osaka University of Pharmaceutical Sciences, Osaka, Japan (K.F.).

DMD Fast Forward. Published on January 8, 2013 as DOI: 10.1124/dmd.112.050344
This article has not been copyedited and formatted. The final version may differ from this version.

Running title: Drug transporters on arachnoid barrier cells

Address correspondence to: Erin G. Schuetz, St Jude Children's Research Hospital, Dept. Pharmaceutical Sciences, 262 Danny Thomas Place, Memphis, TN 38105. Email: erin.schuetz@stjude.org.

Number of text pages: 17

Number of Tables: 1

Number of Figures: 6

Number of references: 34

Number of words in Abstract: 196

Number of words in Introduction: 446

Number of words in Discussion: 1,190

Nonstandard abbreviations used: AB, arachnoid barrier; BBB, blood brain barrier; CP, choroid plexus; BCSFB, blood cerebrospinal fluid barrier.

DMD Fast Forward. Published on January 8, 2013 as DOI: 10.1124/dmd.112.050344
This article has not been copyedited and formatted. The final version may differ from this version.

Abstract

The subarachnoid space, where CSF flows over the brain and spinal cord, is lined on one side by arachnoid barrier (AB) cells that form part of the blood-cerebrospinal fluid (CSF) barrier. However, despite the fact that drugs are administered into the CSF, and CSF drug concentrations are used as a surrogate for brain drug concentration following systemic drug administration, the tight junction AB cells have never been examined for whether they express drug transporters that would influence CSF and CNS drug disposition. Hence, we characterized drug transporter expression and function in AB cells. Immunohistochemical analysis showed P-glycoprotein (Pgp) and BCRP in mouse AB cells, but not other meningeal tissue. The Gene Expression Nervous System Atlas (GENSAT) database and the mouse Allen Brain Atlas confirmed these observations. Microarray analysis of mouse and human arachnoidal tissue revealed expression of many drug transporters and some drug metabolizing enzymes. Immortalized mouse AB cells express functional Pgp on the apical (dura facing) membrane and BCRP on both apical and basal (CSF facing) membranes. Thus, like blood brain barrier (BBB) cells and choroid plexus (CP) cells, AB cells highly express drug transport proteins and likely contribute to the blood-CSF drug permeation barrier.

Introduction

The blood-brain barrier (BBB) (endothelial cells in the veins, arteries, and capillaries of the brain and spinal cord) and the blood-cerebrospinal fluid barrier (BCSFB) (comprised of choroid plexus (CP) epithelial cells, and arachnoid barrier (AB) epithelial cells of the meninges) consist of tight junctioned cells that form physical barriers to CNS and CSF drug penetration (Fig 1) (Saunders et al., 2008). The BBB and CP also express drug transporters that affect drug penetration into the brain (Redzic, 2011). To the best of our knowledge, AB cells have not been characterized previously for drug transporter expression.

The AB cells make up part of the three-layered meninges that cover the brain and spinal cord (Fig 1). The meninges consist of an outermost dura layer (adjacent to the skull), and the two innermost layers (leptomeninges) comprised of the arachnoid mater that includes the tight junctioned arachnoid barrier cells (AB) that sit adjacent to the cerebrospinal fluid (CSF) in the subarachnoid space, and the innermost pia mater, consisting of non-tight junctioned cells lining the brain surface. The AB cell layer has numerous tight junctions and functions as the physiological barrier between the CSF in the subarachnoid space and the fenestrated capillaries in the dura (Schachenmayr and Friede, 1978; Vandenabeele et al., 1996).

Knowledge of drug transporter expression and localization in AB cells bordering the CSF in the subarachnoid space is important for two reasons. First, because a growing number of drugs, including chemotherapies, are administered intrathecally (IT)(into the CSF of the subarachnoid space) by intralumbar injection (Stapleton and Blaney, 2006). For example, a regimen of 13-28 intralumbar chemotherapy injections is standard therapy to eradicate CSF lymphoblasts in childhood acute lymphoblastic leukemia patients because they are at high risk for CNS relapse (Pui et al., 2009). This drug therapy has now fully replaced the more neurotoxic cranial irradiation.

Intrathecal chemotherapy is also used to treat some types of brain and leptomeningeal tumors, and to treat other diseases such as meningitis. It would be expected that drug transporters expressed in AB cells would influence the concentration of intrathecally administered drug that remains in the CSF, their rate of egress from the CSF and, hence, the concentration available to the CNS. Second, the concentration of drugs in the CSF is often used as a surrogate of the unbound drug in the interstitial fluid in the brain and, hence, available to drug targets (Kodaira et al., 2011). Thus, identification of transporters localized in the AB cells adjacent to the CSF space is necessary to correctly interpret exposure-response relationships for CNS acting drugs. The goal of this study was to determine whether drug transporters are expressed in AB cells and their cellular localization and function.

DMD Fast Forward. Published on January 8, 2013 as DOI: 10.1124/dmd.112.050344
This article has not been copyedited and formatted. The final version may differ from this version.

Materials and Methods

Mice. Animal studies were conducted under protocols approved by the St. Jude Children's Research Hospital Committee on the Use and Care of Animals. Female (12-16 wk) Pgp wild type and knock out (CF1) mice (Pippert and Umbenhauer, 2001) and C57BL/6 mice (Charles River, Wilmington, MA) were maintained in a pathogen-free facility. *Abcg2*-EGFP mice have been previously described (Tadjali et al., 2006).

Immunohistochemistry on tissues. Mouse tissue was isolated from Pgp WT and KO and *Abcg2*-EGFP mice. Human brain tissue was obtained from normal brain at autopsy of anonymous donors within 24 hours from the time of death. Tissue was fixed with 10% formalin for 24 h and paraffin sections processed by heat-induced epitope retrieval. Slides were blocked with 5% normal goat serum/PBS for 30 min, followed by overnight incubation with rabbit Anti-Pgp (1:4000) we developed (raised against amino acids 555-575 of human Pgp and immunopurified with the same peptide) or with mouse Anti-Pgp, JSB-1 (1:20) (Abcam, Cambridge, MA) or, or with the rat monoclonal anti-BCRP IgG, BXP-53 (Kamiya Biomedical, Seattle, WA) at 4°C, or anti-GFP IgG (Life Technologies) followed by appropriate secondary antibodies, and detected with the streptavidin-biotin immunoperoxidase method and diaminobenzidine substrate for visualization. After counterstaining with hematoxylin, the slides were mounted. For negative control, the primary antibody was omitted.

***Bcrp* Gene Expression Analysis - Allen Brain Atlas.** *Bcrp* mRNA expression pattern was analyzed at the Allen mouse brain atlas in situ hybridization database (Lau et al., 2008). Allen

Mouse Brain Atlas [Internet]. Seattle (WA): Allen Institute for Brain Science. ©2009. Available from: http//mouse.brain-map.org.

Pgp (*Abcb1a*) gene expression analysis – GENSAT. Localization of Pgp (*Abcb1a*) expression in mouse AB tissue was analyzed at the Gene Expression Nervous System (GENSAT) database ("The Gene Expression Nervous System Atlas (GENSAT) Project, NINDS Contracts N01NS02331 & HHSN271200723701C to The Rockefeller University (New York, NY)" (http://www.gensat.org) (Gong et al., 2003) in *Abcb1a*-EGFP BAC reporter mice in which the EGFP reporter gene is inserted immediately upstream of the coding sequence for Pgp and brain tissue from the mice immunostained with an anti-GFP antibody.

Creation of Immortalized mouse AB cells. Leptomeningeal tissue was isolated from *Abcg2*-GFP male and female mouse embryos (P3), combined, and placed in cold dissociation media (DM) containing 90 mM Na_2S0_4, 30 mM K_2SO_4, 0.25 mM $CaCl_2$, 5.8 mM $MgCl_2$, 10 mM glucose, 1 mM HEPES. Leptomeningeal tissue was centrifuged at 800 X g for 10 min. and dissociated for 25 min. in 37^{o}C DM with 0.0467% collagenase followed by rapid pipetting through a 1 ml pipet, washed in DM and pelleted. Cells were cultured until confluent on poly-D-lysine coated dishes in DMEM with 1% FBS/9% horse serum, fungizone, penicillin/streptomycin (Life Technologies) and glutamine (Murphy et al., 1991). Cells were trypsinized and GFP (+)/CD31 (-) cells were FACS sorted and cultured. At 60% confluence, cells were transduced with an ecotropic lentivirus (manufactured by the St Jude Vector Core Lab) containing the lentiviral plasmid pLOX-T-ag-IRES-TK (Salmon et al., 2000) obtained from the non-profit plasmid repository (Addgene, Cambridge, MA). Four days post transduction cells were transferred to poly-D-lysine coated plates and individual colonies were clonally selected and characterized.

Immunohistochemistry analysis of immortalized mouse AB cells. Immortalized AB Cells were either (a) cultured on 3.0 µm polyester transwell dishes (Corning Inc., Corning, NY) to confluence, or (b) cultured on 35 mm poly-D-lysine glass bottom dishes (BD Biosciences, San Jose, CA) overnight. Cells were fixed with 3.7% formaldehyde in PBS pH 7.4 for 15 min at room temperature followed by 3 X 5 minute washes in PBS. Cells were blocked for 1 h with 2% normal goat serum in PBS followed by a 30 min block in 5% BSA in PBS, incubated for 1 h with primary antibodies in 2% normal goat serum: our rabbit anti-Pgp at 1:500, rat anti-Bcrp (Abcam, BXP-53) at 1:20, rabbit anti-cytokeratin (a "pan" cytokeratin antibody) (DAKO (Carpinteria, CA), Cat. #20622) at 1:20, rabbit anti-Desmoplakin, (Santa Cruz Biotechology (Santa Cruz, CA), Cat. #sc-33555) at 1:50, or rabbit anti-vimentin, (ab92547, Abcam (Cambridge, MA)) at 1:50 . Cells were washed and appropriate secondary antibodies (Alexa Fluor 555-conjugated anti-rat, and anti-rabbit (Life Technologies)) were added at a concentration of 1:500 in 2% normal goat serum for 1 h. Z stack images were acquired using the Marianas system (Intelligent Imaging Innovation (3i), Denver, Colorado), and xz and yz images were acquired to visualize the apical versus basal membrane localization of transporters. Following immunohistochemical staining, the plasma membrane was stained with wheat germ agglutin conjugated to Alexa 594 at a concentration of 5 µg/ml (Invitrogen, Grand Island, NY) for 10 minutes at 22^{o}C. Prolong Gold with DAPI (Invitrogen, Grand Island, NY) was used for mounting.

***MDR1* (Pgp)-EGFP lentivirus transduction of AB cells.** The human *MDR1*-EGFP cDNA (including 62 bases of the 5'-UTR) was PCR amplified from *MDR1*-pEGFP-N1 (kindly provided by Dr. Basil D. Roufogalis, University of Sydney, Australia) (Fu et al., 2004) using the following

primers: FP (with *Sac*II restriction site (italicized)): 5' TCC***CCGCGG***CGTGTACGGTGGGAGGTCTA 3', and RP: 5' GGGAGGTGTGGGAGGTTTT 3'. The human *MDR1*-EGFP cDNA was PCR amplified, purified, and ligated (T4 DNA ligase, Promega) into the restriction digested (*Sac*II and *Not*I) Lenti CL20c-MSCV-EGFP vector (Dr. John Gray, SJCRH) and transformed into Oneshot Top10 competent cells (Invitrogen). Clones were screened by *Sac*II and *Not*I restriction digestion and CL20c-MSCV-Pgp-EGFP positive clones verified by DNA sequencing. The Pgp-EGFP Lentiviral particles were manufactured by Dr. John Gray (St Jude Vector Core). Briefly, HEK293T cells were calcium phosphate co-transfected with the plasmids: CL20c-MSCV-Pgp-EGFP, gagpol (CAGG-HIV gpco), envelope (CAGG-VSVG) and revtat (CAG-RTR2) and three days later, supernatant was harvested, filtered and lentiviral particles titered. Primary mouse AB cells at 60% confluence were transduced with Pgp-EGFP lentiviral particles and 48 h later confocal images were captured by confocal analysis on the Intelligent Imaging Innovations Marianis system.

***In vitro* accumulation assay.** AB cells (50,000 Cells/well) were plated on poly-D-lysine coated 24 well plates for 18 h, treated with inhibitors (5 μM Cyclosporin A or 5 μM fumitremorgin C or 1 µM elacridar (Toronto Research Chemicals, Ontario, Canada)) for 30 min, and then with calcein AM (1 μM) or mitoxantrone (5 μM) or Rhodamine 800 (0.1µM) (Santa Cruz Biotechology, Santa Cruz, CA) for 1 h. Cells were washed with ice cold 1x PBS and harvested. The cellular fluorescence signal of calcein AM (excitation 490nm/emission 520nm) and mitoxantrone (excitation 607nm/emission 684nm) and rhodamine 800 (excitation 682nm/emission 712 nm) were measured with a Synergy H4 Hybrid Multi-Mode Microplate Reader (Biotek, Winooski, VT).

Daunomycin accumulation assay in AB cell cultures. AB cells (50,000) were plated onto the center well of 35 mm poly-D-lysine coated glass bottom dishes and cultured overnight. Cells were preincubated with 5 μM Cyclosporine for 1 h, then 0.5 μM daunomycin was added for 30 min. Images were captured using an Intelligent Imaging Innovations Marianas System, which incorporates a Zeiss Axioplan microscope, a Yokogawa CSUX spinning disk confocal scanhead and a Photometrics Cascade II CCD camera. Daunomycin was excited at 488nm and the emission was collected through a 617/73 bandpass filter, using a 63X 1.4 NA Plan Neofluar objective. The intensity of the intracellular staining was quantified using SlideBook software.

Mouse leptomeningeal tissue microarray analysis. Mouse leptomeningeal tissue from 20-30 neonatal mice (P2) was isolated, combined, and total RNA was prepared using QIAzol Lysis Reagent (Qiagen, Valencia, CA). To remove any genomic DNA contamination, total RNA was treated with the RNase-free DNase (Qiagen) and further purified using RNeasy Mini kit (Qiagen) according to the manufacturer's instructions. The quality of total RNA was monitored by Agilent 2100 Bioanalyzer (Agilent Technologies, Santa Clara, CA, USA). First-strand cDNA was synthesized by use of Superscript II Reverse Transcriptase (Invitrogen, Carlsbad, CA, USA) and T7-Oligo (dT) Primer (Affymetrix, Santa Clara, CA, USA). *In vitro* transcription reactions were performed using a GeneChip IVT Labeling Kit. The labeled cRNA was hybridized to a GeneChip Mouse Genome 430 2.0 Array (Affymetrix). After washing, the arrays were scanned with the GeneChip Scanner 3000 (Affymetrix). Affymetrix Microarray suite (MAS) software (ver. 5.0) was utilized to calculate the signal and *P* values and to set the algorithm's absolute call flag, which indicates the reliability of the data points according to P (present), M (marginal) and A (absent). The data on the chip were scaled to the 500-target intensity value. The prescaled chip data from the

experiment were normalized using GeneSpring GX (ver. 7.3: Agilent Technologies). Normalization with default parameters in GeneSpring software (Per Chip: Normalize to 50th percentile, Per Gene: Normalize to median) was used. Mouse expression values $<1.0 \times 10^2$ are considered low.

Quantitative Real-time PCR (qPCR) analysis. Total cellular RNA was extracted from C57/BL6 mouse tissues using TRIzol (Life Technologies, Grand Island, NY) and cDNA was synthesized from 1 μg of total RNA according to manufacturer's instructions using the iScript cDNA Synthesis Kit (Bio-Rad, Hercules, CA). Q-PCR was performed with specific primers (Supplemental Table 1) using the SYBR Green Master Mix (Life Technologies) according to the manufacturer's instructions and was carried out in an ABI PRISM 7900HT System (Applied Biosystems, Foster City, CA). PCR conditions include initial activation step at 95°C for 15 min, followed by 40 cycles in which each cycle consisted of denaturation at 92°C for 30 s, annealing for 30 s, and synthesis at 72°C for 60 s. Specificity of amplification was confirmed in each case by performing melt curve analysis. To minimize the effect of sample handling differences, all results were calculated as ΔCt (the Ct (threshold cycle) value for any gene of interest - Ct of the endogenous housekeeping gene glyceraldehyde-3-phosphate dehydrogenase (GAPDH)).

Results

Pgp is expressed at the apical membrane of arachnoid barrier cells of mouse, monkey and human leptomeninges. Immunohistochemical (IHC) staining revealed Pgp in endothelial cells that comprise the BBB in the veins, arteries, and capillaries throughout the brain and spine of Pgp wild-type (WT) but not KO mice (Fig. 2A-E). Pgp was also expressed in AB cells in the brain and spinal cord, and Pgp's staining intensity was at least equal to that in the endothelial cells comprising the BBB. Further confirmation of Pgp leptomeningeal expression came from evaluating a BAC transgenic mouse that used the endogenous mouse *Abcb1a* promoter to drive EGFP reporter expression. This mouse was previously generated as part of the Gene Expression Nervous System Atlas (www.Gensat.org) project. IHC for EGFP in mouse brain (Fig. 2F) and spinal cord (Fig. 2G) found Pgp expression in the endothelial cells in the veins, arteries, and capillaries of the brain and spinal cord and in the leptomeninges. The Gensat site identifies Pgp in Pia cells, however this is incorrect, because an extensive review of numerous slides of mouse brain revealed Pgp immunostaining only in AB cells, not pia cells (Fig. 2A,C, D).

Immunohistochemical staining of human meninges with JSB-1 monoclonal antibody (used for Pgp clinical diagnostics) (Fig. 2H) and with rabbit Pgp IgG (Fig. 2I) revealed an identical pattern of Pgp immunostaining in the BBB and AB cells. Monkey AB cells were also positive for Pgp (Fig. 2K). There was no staining for Pgp in the arachnoid reticular cell layer or trabecular cells or in the pia mater in monkey or human tissue. Compared to the closely associated pia-arachnoidal membranes in the mouse, the human (and monkey) arachnoid membrane is characterized by a relatively thick reticular cell layer with trabecular cells (strands of connective tissue connecting pia and AB) that clearly separates the AB cell layer from the pia mater.

DMD Fast Forward. Published on January 8, 2013 as DOI: 10.1124/dmd.112.050344
This article has not been copyedited and formatted. The final version may differ from this version.

The anatomy of the arachnoid barrier layer shows a continuous basal lamina on its inner surface facing the CSF and the innermost loosely organized arachnoid reticular cell layer that traverses the subarachnoid space between the AB cells and the pia cells on the surface of the brain (Schachenmayr and Friede, 1978; Vandenabeele et al., 1996). By definition, the surface of the AB cell forming the base and contacting the basement membrane (and facing the CSF) is the basal surface. Increased magnification of Pgp IHC of mouse and monkey brain (Fig. 2J,K) demonstrated prominent staining on the apical membrane of AB cells facing the dura.

The localization and expression of Pgp in CP and ependymal cells is controversial (Gazzin et al., 2008; Rao et al., 1999; Roberts et al., 2008). Immunostaining of Pgp WT and KO mice CP revealed an identical non-specific punctate and granular staining pattern throughout the cytoplasm (Fig. 3A,B) of mice with both genotypes. At a lower concentration of primary antibody (Fig. 3C), Pgp was stained in the BBB, but staining was absent in the ependymal cells and only weakly present in some CP cells.

BCRP is highly expressed in mouse AB cells. BCRP immunostaining was readily detected in mouse AB cells and blood vessel endothelium (Fig. 4A). The expression pattern of BCRP was confirmed using a mouse containing the *Abcg2*-IRES (internal ribosomal entry)-EGFP allele (IRES-EGFP is inserted downstream of the *Abcg2* stop codon). This allelic modification results in expression of the EGFP reporter gene under control of the *Abcg2* transcriptional regulatory elements, with coexpression of a functional wild-type BCRP protein (Tadjali et al., 2006). Immunohistochemistry detected EGFP expression in the mouse AB cells but not in pia cells (Fig. 4B,C). Final verification of *Bcrp*'s mRNA expression pattern comes from the Allen mouse brain atlas in situ hybridization database (http://mouse.brain-map.org/) (Fig. 4D,E). Expression of

Abcg2 is higher in the arachnoid meningeal tissue then in virtually all other brain regions. However, whether the same is true in AB tissue from other species, including humans, remains to be determined.

Establishment of immortalized mouse AB cell lines. The leptomeninges were dissected from *Abcg2*-IRES-EGFP mice (age P3), cells were isolated by collagenase digestion, then cultured for four days and AB cells were isolated by FACs (cells positive for GFP and negative for the blood vessel endothelial marker CD31). Since primary AB cultures rapidly senesce after 4-5 passages, lentivector transfer of pLOX-Tag-iresTK was used to immortalize the primary cells (Salmon et al., 2000). The morphology of the primary (not shown) and SV40 Tag immortalized cells was identical with large nuclei and a more spindle-like appearance at low density (Fig. 5A) and a cobblestone appearance at higher density. The AB cells had strong positive immunostaining for cytokeratin (cytoplasmic and displaying long filaments and a basketlike structure indicative of cytokeratin organization) (Fig. 5B), desmoplakin (with the strongest expression between cells being indicative of its role as an obligate component of functional desmosomes) (Fig. 5C), and the intermediate filament protein vimentin (primarily seen in juxtanuclear knots) (Fig. 5D). The co-expression of these three proteins identifies them as AB cells (Janson et al., 2011; Murphy et al., 1991) and eliminates the possibility that the cells are contaminated with endothelial cells, fibroblasts, astrocytes or macrophages (Murphy et al., 1991). The cells were also stained intensely positive for prostaglandin D2 synthase (Fig. 5E), a protein known to be highly expressed in AB cells (Beuckmann et al., 2000; Fujimori et al., 2007).

Pgp and BCRP immunolocalization and function in cultured AB cells. The subcellular distribution of Pgp and BCRP was determined in AB cells in transwell culture. Examination of the cells at a plane perpendicular to the transwell culture dish showed endogenous Pgp most highly expressed at the apical membrane (Fig. 6A). Further confirmation that Pgp is apically expressed was determined by transducing the cells in Figure 6B with a lentivirus expressing a Pgp-EGFP fusion protein (Fu et al., 2004). Co-expression of the Pgp-EGFP (green) with a plasma membrane stain (red) to the apical membrane was revealed by yellow co-staining (Fig. 6B). We first attempted to verify transporter function by measuring directional transport of a Pgp or Bcrp substrate across mouse AB cells in transwell culture. Unfortunately, we were unable to sustain high TEER values in order to generate consistent transport results in transwell culture. To verify Pgp transporter function, AB cells were incubated with the Pgp substrate daunomycin (Fig. 6C) or calcein AM (Fig. 6D) or rhodamine 800 (On et al., 2011) in the presence or absence of the inhibitor cylosporin A (CsA) (at a concentration (1μM) that should inhibit only Pgp) or elacridar (a dual Pgp/Bcrp inhibitor). The intracellular accumulation of each Pgp substrate was reproducibly increased in the presence of the Pgp inhibitor. Pretreatment with neither the Bcrp inhibitor FTC (fumitremorgin C), nor the MRP inhibitor MK571, had any effect on retention of rhodamine 800 (data not shown).

In contrast to Pgp, endogenous BCRP immunostaining was equal at the apical and basal membranes (with some cytoplasmic staining) of all AB cells on polylysine glass dishes (Fig. 6E) or in transwell culture (Fig. 6F) Preincubation of AB cells with the BCRP inhibitor FTC increased intracellular mitoxantrone fluorescence up to 2.5-fold (Fig. 6G). Thus, immortalized cultures of mouse AB cells retain membrane expression of functional Pgp and BCRP.

Microarray analysis of drug detoxification genes in arachnoid barrier leptomeninges.

Mouse leptomeningeal mRNA expression of drug uptake and efflux transporters, cytochromes P450, the nuclear hormone receptors *PXR* and *CAR*, and the AB marker prostaglandin D2 synthase was analyzed by microarray and compared with that of normal adult human arachnoid mRNA expression (Gene Expression Omnibus) (Table 1). Both *MDR1* and *BCRP* were highly expressed in human and mouse tissue. The monocarboxylate transporter *MCT1* was the most highly expressed drug transporter in mouse, but lower in human. This transporter is also known to interact with drugs such as simvastatin and valproate (Anderson and Thwaites, 2010). *SLCO1C1*, an organic anion transporter highly expressed at the BBB (and previously called BBB-specific anion transporter 1), was also expressed in mouse leptomeningeal tissue. Methotrexate SLC uptake transporters (*OAT1, OAT3* and the reduced folate carrier (*SLC19A1*)) (VanWert and Sweet, 2008; Zhao et al., 2011) were expressed in AB tissue from both species. Human leptomeninges had detectable expression of the nuclear hormone receptor *PXR* (*NR1I2*), while *CAR* (*Nr1I3*) was more highly expressed in mouse leptomeninges. *CYP1B1* and *CYP4A* were the most abundant CYPs in AB cells from both species. Quantitative real-time PCR of mouse leptomeninges, CP and whole brain pooled from day 2 neonatal mice was used to evaluate and confirm microarray gene expression data (Table 1). The lower the ΔCt value, the higher the expression of the gene of interest. In total the results showed that, like BBB and CP (Decleves et al., 2011), AB cells express a variety of drug detoxification genes. Moreover, the expression pattern of transporters in the *epithelial* AB cells is closer to that of the other BCSF barrier cells - the *epithelial* CP cells (e.g., higher expression of Oat1/OAT1 and Oat3/OAT3), rather than BBB blood vessel *endothelial* cells

Discussion

Almost two decades after it was first demonstrated that BBB expressed Pgp has a protective role in excluding drugs from the brain (Schinkel et al., 1994), and that CP Pgp functions as a drug-permeability barrier (Rao et al., 1999), we report that AB cells represent another blood-CSF drug transport barrier expressing functional drug transporters such as Pgp and BCRP. Transporter expression in AB cells in the cranial and spinal meninges makes mechanistic sense because, like CP, the fenestrated capillaries in the dura lack barrier properties and the barrier function shifts to the AB epithelial layers. Moreover, Affymetrix GeneChip array analysis of mouse and human arachnoid barrier tissue revealed expression of additional uptake and efflux transporters, and that AB cells have a CYP enzymatic barrier.

There are four distinct blood-CSF interfaces: the CP, the AB, the ependymal cells separating the ventricular system from the extracellular fluid of the brain, and the pia leptomeningeal cells on the brain surface (Johanson et al., 2011). Our studies suggest that Pgp in the AB membrane is a primary drug efflux barrier at the blood-CSF interface. First, we, and others (Roberts et al., 2008), did not detect Pgp in either pia leptomeningeal cells or ependymal cells. Ependymal cell Pgp immunostaining has been reported (King et al., 2001), but it is difficult to reconcile why ependymal cells, that lack tight junctions to restrict the free exchange of drugs between the CSF and brain tissue, would express a drug transporter. In addition, the expression level and cellular localization of Pgp in CP has been reported to be cytoplasmic (Miller, 2004), or at the subapical membrane (Rao et al., 1999), or low to nonexistent (Baehr et al., 2006; Roberts et al., 2008). In contrast, Pgp immunostaining in AB was at least equivalent to its immunostaining intensity at the BBB. Drug transporter expression in AB cells has likely been missed to date because the AB layer is frequently detached from the brain by skull removal. This occurs because,

even within days after birth, the dura increasingly attaches to the skull. The result is that if care is not taken, when the skull is removed from the brain, tissue above the CSF space (arachnoid tissue and dura) is retained with the skull.

Creation of an immortalized AB cell model was essential to elucidation of AB function. These cells polarize and retain key morphological AB features including cytokeratin, desmoplakin, and vimentin, and high expression of prostaglandin D2 synthase. They also preserve Pgp and Bcrp transporter localization and function as shown by export of transporter typical substrates such as mitoxantrone, calcein AM, rhodamine 800, and daunomycin. Most importantly, cultured AB cells expressed Pgp and BCRP at the membrane. Pgp was expressed on the apical surface of cultured AB cells, consistent with a more intense Pgp apical immunostaining on AB tissue from mouse and monkey brain. Although the apical surface of many cells faces a lumen, the AB apical surface faces the dura, and the basal surface faces the CSF.

Pgp expression on the apical membrane of AB cells is likely an important component of the blood-CSF barrier preventing the CSF entry of systemic drugs that easily leave the leaky fenestrated dural capillaries. In addition, it would enhance removal of drugs that get into the CSF either by secretion from the brain interstitial fluid compartment, or following an intrathecal drug administration. Although our studies were performed in mice, anecdotal evidence supporting a role for apical membrane Pgp having a barrier function comes from an MRI study of human brain 90 min. after systemic administration of ^{99}mTc-sestamibi (Rao et al., 1999), a Pgp substrate. There was an intense MRI signal localized in the CP (but none in the CSF or brain parenchyma) and around the brain periphery. Our results suggest that the peripheral signal may represent ^{99}mTc-sestamibi that left the fenestrated dural capillaries, infiltrated the dura and that AB Pgp is preventing it from penetrating into the CSF.

The dual expression of BCRP on both apical and basal surface of AB cells is unique – there are no other cell types where BCRP is reportedly expressed on both cell membranes. This implies that BCRP has two distinct functions in the AB cells. BCRP on the apical AB membrane likely forms part of the blood-CSF drug transport barrier preventing CSF penetration of systemic drugs. Conversely, BCRP on the basal AB membrane would increase the CSF retention of substrates, such as topotecan and methotrexate that can be administered intrathecally.

The finding that BCRP faces the CSF subarachnoid space in both types of blood-CSF barrier cells, CP (Zhuang et al., 2006) and AB, suggests that BCRP may have an important function in secreting some factor produced in these cells into the CSF. The CSF is a regulator of neurogenesis and behavior (Zappaterra and Lehtinen, 2012) and CP and AB cells produce micronutrients, neurotrophins, growth factors, retinoic acid and prostaglandins that are secreted into the CSF. Although BCRP is known to transport endogenous vitamins such as riboflavin (vitamin B_2), folic acid (folate, vitamin B_9) and vitamin K_3 (Vlaming et al., 2009), the physiological function and endogenous substrate secreted into the CSF by BCRP remains to be determined.

Our studies have strong implications for using CSF as a surrogate for brain exposure following systemic administration of BCRP and Pgp substrates (Xiao et al., 2012). For Pgp substrates, conventional knowledge posits that CSF drug concentration is only influenced by BBB and CP Pgp (Kodaira et al.). Our studies put forth a new paradigm: CSF drug concentration is strongly influenced by AB Pgp and BCRP. Pharmacokinetic quantification of brain drug exposure by using CSF will only be as good as the models, which currently do not incorporate the cranial and spinal AB surface area and drug transporters, or the apical or basal expression of these transporters. Moreover, by our calculations the total meninges surface area (0.27 m^2)= [cranial

DMD Fast Forward. Published on January 8, 2013 as DOI: 10.1124/dmd.112.050344
This article has not been copyedited and formatted. The final version may differ from this version.

meninges (0.17 m^2) + spinal meninges (0.02 m^2) + arachnoid granulations (0.078 m^2)], actually exceeds the CP surface area (0.021 m^2). Given the clear evidence for intersite differences in CNS pharmacokinetics of Pgp and BCRP substrates, and the difficulty in modeling the impact of the drug transporters on drug concentration in each compartment, improved models are needed to quantitatively evaluate the individual contribution of Pgp and BCRP at the BBB, CP and AB to brain and CSF concentrations.

In conclusion, AB cell expression of drug transporters adds to the increasing recognition of the complexity of transporters of the blood-brain and blood-CSF barriers. This finding is important because (1) a growing number of drugs, including chemotherapeutics, are administered into the CSF by intrathecal injection. It would be expected that drug transporters expressed in AB cells would influence the rate of drug egress from the CSF and the concentration of drug that remains in the CSF; and (2) the concentration of drugs in the CSF is often used as a surrogate of the unbound drug in the interstitial fluid in the brain. Hence, identification of transporters localized in the AB cells adjacent to the CSF space is necessary to correctly interpret exposure-response relationships for brain and CSF concentrations of Pgp and BCRP substrates which includes many chemotherapeutics.

Acknowledgements. We gratefully acknowledge the technical support of St Jude Children's Research Hospital: Small Animal Imaging Resource, the Cellular Imaging Shared Resource, the Veterinary Pathology Core, and the Hartwell Center for oligonucleotide synthesis; Drs. Richard and Michelle Smeyne (SJCRH) for training on isolation of mouse leptomeningeal tissue.

DMD Fast Forward. Published on January 8, 2013 as DOI: 10.1124/dmd.112.050344
This article has not been copyedited and formatted. The final version may differ from this version.

Author Contributions:

Participated in research design: Schuetz, Yasuda, Cline, Ekins, Sorrentino

Conducted experiments: Yasuda, Cline, Onciu, Thirumaran, Fujimori

Contributed new reagents or analytic tools: Fatima, Sorrentino, Urade

Performed data analysis: Schuetz, Yasuda, Cline, Vogel, Onciu, Fujimori

Wrote or contributed to the writing of the manuscript: Schuetz, Yasuda, Cline, Vogel, Ekins, Fujimori, Urade

References

Anderson CM and Thwaites DT (2010) Hijacking solute carriers for proton-coupled drug transport. *Physiology (Bethesda)* **25**(6): 364-377.

Baehr C, Reichel V and Fricker G (2006) Choroid plexus epithelial monolayers--a cell culture model from porcine brain. *Cerebrospinal Fluid Research* **3**: 13.

Beuckmann CT, Lazarus M, Gerashchenko D, Mizoguchi A, Nomura S, Mohri I, Uesugi A, Kaneko T, Mizuno N, Hayaishi O and Urade Y (2000) Cellular localization of lipocalin-type prostaglandin D synthase (beta-trace) in the central nervous system of the adult rat. *The Journal of Comparative Neurology* **428**(1): 62-78.

Decleves X, Jacob A, Yousif S, Shawahna R, Potin S and Scherrmann JM (2011) Interplay of drug metabolizing CYP450 enzymes and ABC transporters in the blood-brain barrier. *Current Drug Metabolism* **12**(8): 732-741.

Fu D, Bebawy M, Kable EP and Roufogalis BD (2004) Dynamic and intracellular trafficking of P-glycoprotein-EGFP fusion protein: Implications in multidrug resistance in cancer. *International Journal of Cancer Journal International du Cancer* **109**(2): 174-181.

Fujimori K, Watanabe M, Urade Y and Ishikawa K (2007) Increased production of lipocalin-type prostaglandin D synthase in leptomeningeal cells through contact with astrocytes. *Neuroscience Letters* **423**(2): 133-137.

Gazzin S, Strazielle N, Schmitt C, Fevre-Montange M, Ostrow JD, Tiribelli C and Ghersi-Egea JF (2008) Differential expression of the multidrug resistance-related proteins ABCb1 and ABCc1 between blood-brain interfaces. *The Journal of Comparative Neurology* **510**(5): 497-507.

Gong S, Zheng C, Doughty ML, Losos K, Didkovsky N, Schambra UB, Nowak NJ, Joyner A, Leblanc G, Hatten ME and Heintz N (2003) A gene expression atlas of the central nervous system based on bacterial artificial chromosomes. *Nature* **425**(6961): 917-925.

Janson C, Romanova L, Hansen E, Hubel A and Lam C (2011) Immortalization and functional characterization of rat arachnoid cell lines. *Neuroscience* **177**: 23-34.

Johanson C, Stopa E, McMillan P, Roth D, Funk J and Krinke G (2011) The distributional nexus of choroid plexus to cerebrospinal fluid, ependyma and brain: toxicologic/pathologic phenomena, periventricular destabilization, and lesion spread. *Toxicologic Pathology* **39**(1): 186-212.

King M, Su W, Chang A, Zuckerman A and Pasternak GW (2001) Transport of opioids from the brain to the periphery by P-glycoprotein: peripheral actions of central drugs. *Nature Neuroscience* **4**(3): 268-274.

Kodaira H, Kusuhara H, Fujita T, Ushiki J, Fuse E and Sugiyama Y (2011) Quantitative evaluation of the impact of active efflux by p-glycoprotein and breast cancer resistance protein at the blood-brain barrier on the predictability of the unbound concentrations of drugs in the brain using cerebrospinal fluid concentration as a surrogate. *The Journal of Pharmacology and Experimental Therapeutics* **339**(3): 935-944.

Lau C, Ng L, Thompson C, Pathak S, Kuan L, Jones A and Hawrylycz M (2008) Exploration and visualization of gene expression with neuroanatomy in the adult mouse brain. *BMC Bioinformatics* **9**: 153.

Miller DS (2004) Confocal imaging of xenobiotic transport across the choroid plexus. *Advanced Drug Delivery Reviews* **56**(12): 1811-1824.

Murphy M, Chen JN and George DL (1991) Establishment and characterization of a human leptomeningeal cell line. *Journal of Neuroscience Research* **30**(3): 475-483.

On NH, Chen F, Hinton M and Miller DW (2011) Assessment of P-glycoprotein activity in the blood-brain barrier (BBB) using near infrared fluorescence (NIRF) imaging techniques. *Pharm Res* **28**:2505-2515.

Pippert TR and Umbenhauer DR (2001) The subpopulation of CF-1 mice deficient in P-glycoprotein contains a murine retroviral insertion in the mdr1a gene. *Journal of Biochemical and Molecular Toxicology* **15**(2): 83-89.

Pui CH, Campana D, Pei D, Bowman WP, Sandlund JT, Kaste SC, Ribeiro RC, Rubnitz JE, Raimondi SC, Onciu M, Coustan-Smith E, Kun LE, Jeha S, Cheng C, Howard SC, Simmons V, Bayles A, Metzger ML, Boyett JM, Leung W, Handgretinger R, Downing JR, Evans WE and Relling MV (2009) Treating childhood acute lymphoblastic leukemia without cranial irradiation. *The New England Journal of Medicine* **360**(26): 2730-2741.

Rao VV, Dahlheimer JL, Bardgett ME, Snyder AZ, Finch RA, Sartorelli AC and Piwnica-Worms D (1999) Choroid plexus epithelial expression of MDR1 P glycoprotein and multidrug resistance-associated protein contribute to the blood-cerebrospinal-fluid drug-permeability barrier. *Proceedings of the National Academy of Sciences of the United States of America* **96**(7): 3900-3905.

Redzic Z (2011) Molecular biology of the blood-brain and the blood-cerebrospinal fluid barriers: similarities and differences. *Fluids and Barriers of the CNS* **8**(1): 3.

Roberts LM, Black DS, Raman C, Woodford K, Zhou M, Haggerty JE, Yan AT, Cwirla SE and Grindstaff KK (2008) Subcellular localization of transporters along the rat blood-brain barrier and blood-cerebral-spinal fluid barrier by in vivo biotinylation. *Neuroscience* **155**(2): 423-438.

Salmon P, Oberholzer J, Occhiodoro T, Morel P, Lou J and Trono D (2000) Reversible immortalization of human primary cells by lentivector-mediated transfer of specific genes. *Molecular Therapy* **2**(4): 404-414.

Saunders NR, Ek CJ, Habgood MD and Dziegielewska KM (2008) Barriers in the brain: a renaissance? *Trends in Neurosciences* **31**(6): 279-286.

Schachenmayr W and Friede RL (1978) The origin of subdural neomembranes. I. Fine structure of the dura-arachnoid interface in man. *The American Journal of Pathology* **92**(1): 53-68.

Schinkel AH, Smit JJ, van Tellingen O, Beijnen JH, Wagenaar E, van Deemter L, Mol CA, van der Valk MA, Robanus-Maandag EC, te Riele HP and et al. (1994) Disruption of the mouse mdr1a P-glycoprotein gene leads to a deficiency in the blood-brain barrier and to increased sensitivity to drugs. *Cell* **77**(4): 491-502.

Stapleton S and Blaney S (2006) New agents for intrathecal administration. *Cancer Investigation* **24**(5): 528-534.

Tadjali M, Zhou S, Rehg J and Sorrentino BP (2006) Prospective isolation of murine hematopoietic stem cells by expression of an Abcg2/GFP allele. *Stem Cells* **24**(6): 1556-1563.

Vandenabeele F, Creemers J and Lambrichts I (1996) Ultrastructure of the human spinal arachnoid mater and dura mater. *Journal of Anatomy* **189 (Pt 2)**: 417-430.

VanWert AL and Sweet DH (2008) Impaired clearance of methotrexate in organic anion transporter 3 (Slc22a8) knockout mice: a gender specific impact of reduced folates. *Pharmaceutical Research* **25**(2): 453-462.

Vlaming ML, Lagas JS and Schinkel AH (2009) Physiological and pharmacological roles of ABCG2 (BCRP): recent findings in Abcg2 knockout mice. *Advanced Drug Delivery Reviews* **61**(1): 14-25.

Xiao G, Black C, Hetu G, Sands E, Wang J, Caputo R, Rohde E and Gan LS (2012) Cerebrospinal fluid can be used as a surrogate to assess brain exposures of breast cancer resistance protein and P-glycoprotein substrates. *Drug Metabolism and Disposition* **40**(4): 779-787.

Zappaterra MW and Lehtinen MK (2012) The cerebrospinal fluid: regulator of neurogenesis, behavior, and beyond. *Cellular and Molecular Life Sciences*.

Zhao R, Diop-Bove N, Visentin M and Goldman ID (2011) Mechanisms of membrane transport of folates into cells and across epithelia. *Annual Review of Nutrition* **31**: 177-201.

Zhuang Y, Fraga CH, Hubbard KE, Hagedorn N, Panetta JC, Waters CM and Stewart CF (2006) Topotecan central nervous system penetration is altered by a tyrosine kinase inhibitor. *Cancer Research* **66**(23): 11305-11313.

Footnotes

*Authorship note: Dr. Yasuda and Ms. Cline contributed equally to this work.

The work was supported by the United States National Institutes of Health Cancer Center Support Grant [Grant P30 CA21765] and by Cancer Center Developmental Funds, and by the American Lebanese Syrian Associated Charities.

Mihaela Onciu's present address is: OncoMetrix, Memphis, TN, USA.

Send reprint requests to: Erin G. Schuetz, St Jude Children's Research Hospital, Dept. Pharmaceutical Sciences, 262 Danny Thomas Place, Memphis, TN 38105. Email: erin.schuetz@stjude.org.

DMD Fast Forward. Published on January 8, 2013 as DOI: 10.1124/dmd.112.050344
This article has not been copyedited and formatted. The final version may differ from this version.

Figure Legends

Figure 1. Arachnoid barrier (AB) cell - CSF interface. Meninges comprised of pia mater (on the brain surface and lining one side of CSF in the subarachnoid space), arachnoid barrier cells (sandwiching one side of the CSF space), and the dura mater containing fenestrated (leaky) capillaries. Expression and location of drug transporters determined from this manuscript (A). Coronal section of the brain showing the three drug transporter barrier cells: BBB, choroid plexus and AB cells relative to the CSF produced by the choroid plexus and circulating in the subarachnoid space (B).

Figure 2. Pgp is highly expressed in brain and spinal cord AB cells. Immunochemical staining using an anti-Pgp antibody shows Pgp expression (solid arrowhead) in AB cells and in blood vessel endothelial cells of the blood brain barrier (BBB) in the brain and spine, respectively, of Pgp WT mice (A, C, D), and its absence in Pgp KO mice (B, E). GFP immunostaining (solid arrowhead) in the meninges of BAC *abcb1a*-EGFP reporter mice at day e15.5 in a sagittal head section (F) and in adult spine (G) (images "The Gene Expression Nervous System Atlas (GENSAT) Project, NINDS Contracts N01NS02331 & HHSN271200723701C to The Rockefeller University (New York, NY)." Pgp immunostaining (solid arrowhead) in human arachnoid barrier cells using JSB-1 (H) and rabbit anti-Pgp antibodies (I). Pgp immunostaining (solid arrowhead) is more intense on the apical membranes of mouse (J) and monkey (K) AB cells. Arachnoid reticular cell layer and trabeculae (asterisk) - visible in human and monkey (H, I, K) meninges.

Figure 3. Pgp expression in mouse choroid plexus. Immunostaining for Pgp in choroid plexus of Pgp WT (A, C) and KO (B) mice.

Figure 4. Bcrp expression in mouse AB cells. Immunostaining of BCRP in AB cells of mouse meninges with anti-BCRP-IgG (BXP-53) (A). Immunostaining of GFP in AB cells of *Abcg2*-promoter_EGFP reporter mice at low (B) and high (C) magnification. *In situ* hybridization for *Bcrp* expression in a sagittal section of mouse brain at low (D) and high (E) magnification - images from the Allen Institute for Brain Science (http://mouse.brain-map.org).

Figure 5. **Characterization of mouse immortalized arachnoid barrier cell cultures.** Phase contrast microscopy of AB cells at early passage (A). Confocal analysis of mouse AB cells in transwell culture incubated with antibodies against cytokeratin (B), desmoplakin (C), vimentin (D), and prostaglandin D2 synthase (E) and revealed (red staining) with appropriate secondary antibodies. Cell nuclei were counterstained with DAPI (4', 6-diamindino-2-phenylindole).

Figure 6. Pgp and BCRP localization and function in immortalized mouse AB cells. Confocal analysis of endogenousPgp (A) and BCRP (E, F) (immunostained in red with nucleic acids stained with DAPI) in cultured AB cells. The top view of the cells is the largest panel and the upper and left panels show an optical section perpendicular to the plane of the cell layer. Confocal analysis of AB cells transduced for 48 h with a Pgp-EGFP (green) fusion lentivirus followed by plasma membrane chemical staining (red) shows apical co-staining (yellow) of Pgp-EGFP and plasma membrane (B). Daunomycin (C) and calcein AM (1μM) and rhodamine 800 (Ro800, 0.1μM) (D) fluorescence in AB cells cultured in the absence or presence of cyclosporin A (CsA) or 1μM

elacridar (ECD). Mitoxantrone fluorescence in AB cells in the absence or presence of 5 μM Fumitremorgin C (FTC) (G). Cellular fluorescence values for substrate alone (set at 1)(± SD) were compared to values in the presence of inhibitors using a Student's *t*-test (2-sided) with ** statistically different from substrate alone at $P < 0.01$.

DMD Fast Forward. Published on January 8, 2013 as DOI: 10.1124/dmd.112.050344
This article has not been copyedited and formatted. The final version may differ from this version.

Table 1. ADME gene expression in mouse brain and human arachnoid tissue

Mouse leptomeninges[a]	x10^2	Mouse LM (ΔCt)[b]	Mouse CP (ΔCt)[c]	Mouse Brain (ΔCt)[d]	Human Arachnoid[e]	x10^3	Example Human substrates/ligands
L-Ptgds	73.4	-6.01 (1)	1.34 (1)	1.75 (1)	*L-PTGDS*	1,371	
Beta-actin	59.1				*Zona Occludens 1*	78.2	
Slc16a1/Mct1	27.9				*CYP1B1*	73.4	Retinal, Arachidonic acid
Slco1c1/Oatp-f	17.3				*CYP4A11*	38.8	Fatty acids (medium chain)
Cyp1b1	12.9	2.63 (4)	7.04 (4)	9.38 (7)	*ABCB1/MDR1*	28.5	Hydrocortisone
Slc22a6/Oat1	10.9	0.28 (2)	8.30 (6)	10.25 (8)	*SLC22A2/OCT1*	24	Nucleoside analogs
Abcg2/Bcrp	10.8	3.22 (5)	7.61 (5)	6.54 (2)	*SLC22A6/OAT1*	15.8	Methotrexate
Slc22a8/Oat3	9.2	1.80 (3)	4.78 (2)	7.61 (4)	*SLC22A8/OAT3*	6.9	Methotrexate
Abcb1a/Mdr1a	6.2	3.89 (6)	6.15 (3)	7.58 (3)	*CYP3A5*	6.4	Tacrolimus
Abcc4/Mrp4	2.1	6.16 (7)	8.49 (7)	9.28 (6)	*ABCG2/BCRP*	4.7	Topotecan
Slco1a4/Oatp2	1.6				*CYP2D6*	4.4	Tamoxifen
Nr1i3/Car	1.1	15.96 (9)	12.60 (9)	16.51 (9)	*SLC16A1/MCT1*	4.4	Lactate, Glucose
Abcb6/Prp	1.1				*ABCB6/PRP*	4.1	Porphyrin
Slc16a11/Mct11	0.9				*SLC19A1/RFC1*	2.8	Methotrexate
Abcc1/Mrp1	0.9	7.18 (8)	9.54 (8)	8.43 (5)	*SLC16A11*	1.5	Monocarboxylates
Cyp2d22	0.6				*NR1I2/PXR*	1.2	Rifampin
Abcc3/Mrp3	0.2				*CYP2B6*	1.2	Cyclophosphamide

[a]**Mouse Leptomeninges** from day 2 neonates; Mouse expression values <1.0 x 10^2 are considered low

[b,c,d] The ΔCt values for genes of interest (rank order in parentheses) obtained from qPCR analysis of mouse [b]leptomeninges (LM), [c]choroid plexus (CP), and [d]whole brain pooled from day 2 neonates

[e]**Human arachnoid membrane** expression – average value from two normal human arachnoid membranes (GEO dataset: GSE19727).

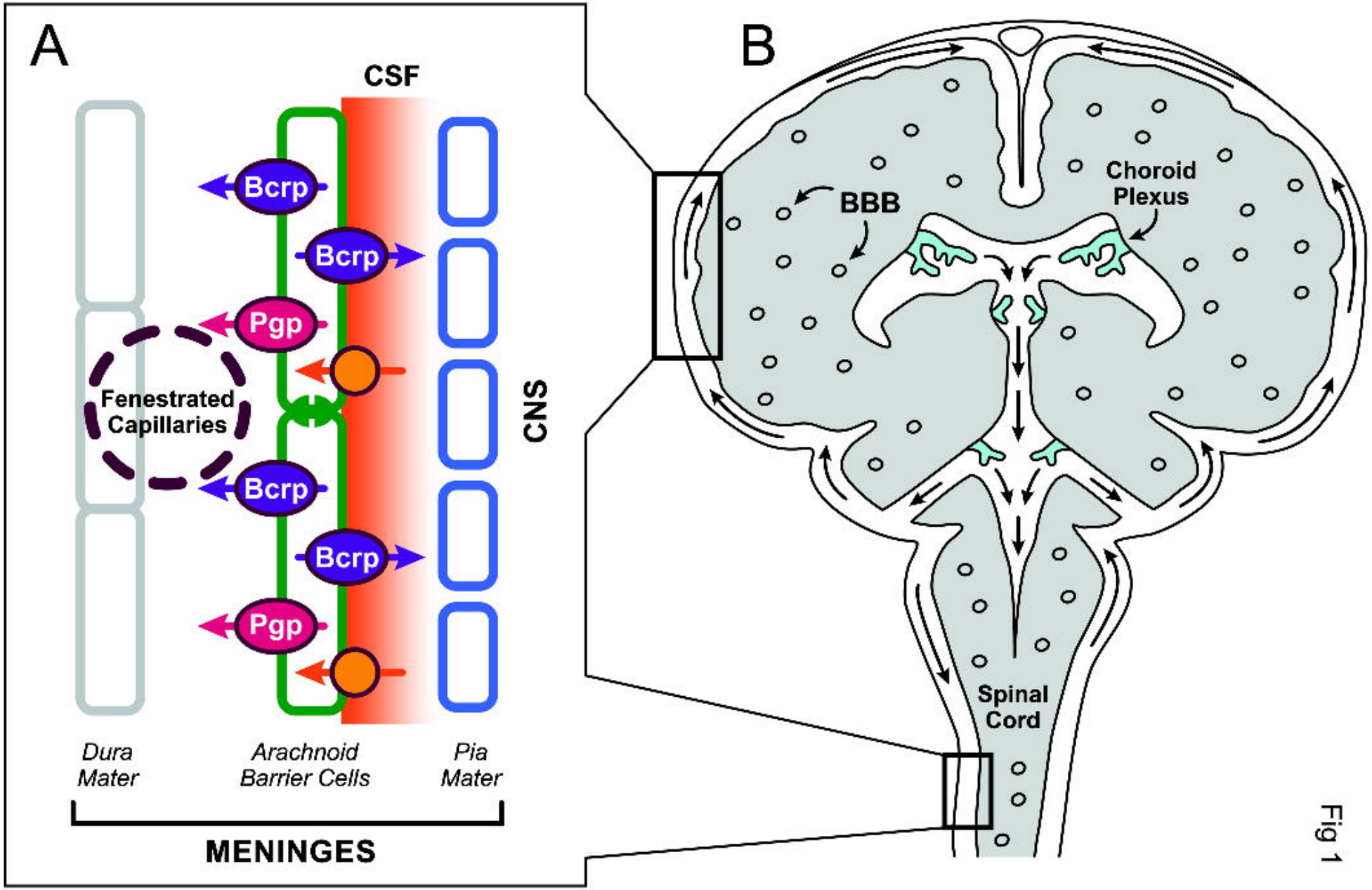
A
CSF
Bcrp
Bcrp
Pgp
Fenestrated Capillaries
Bcrp
Bcrp
Pgp
CNS
Dura Mater
Arachnoid Barrier Cells
Pia Mater
MENINGES
B
BBB
Choroid Plexus
Spinal Cord

Fig 1

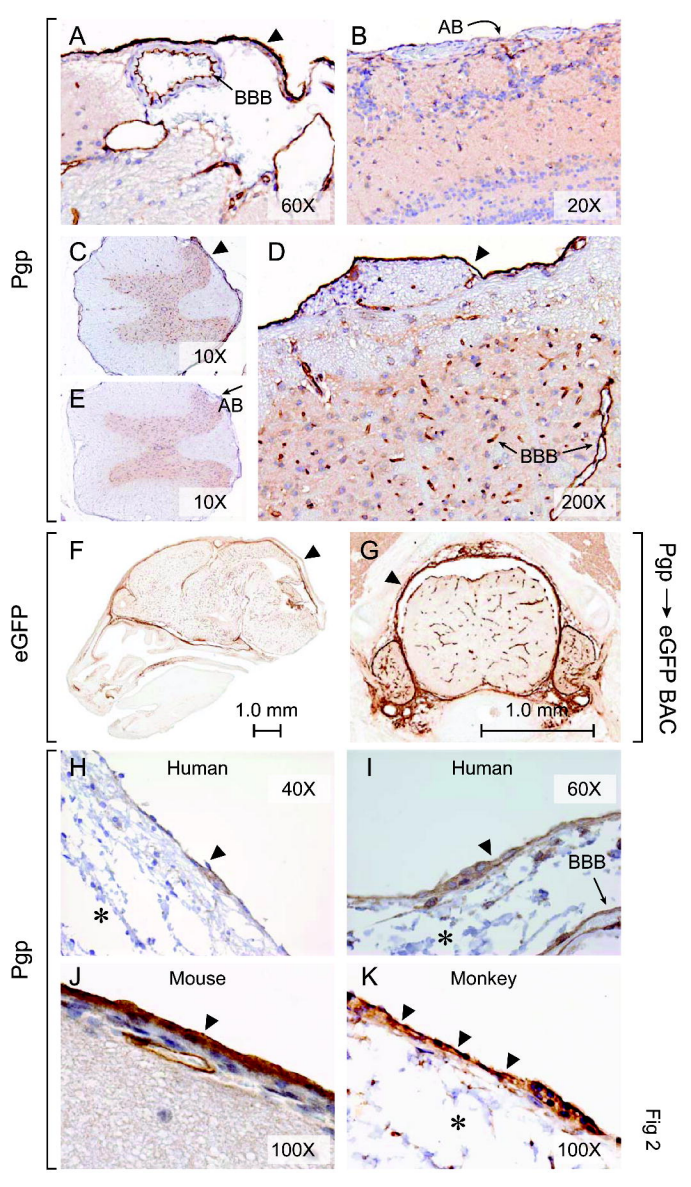
A
BBB
60X
B
AB
20X
Pgp
C
10X
D
BBB
200X
E
AB
10X
F
1.0 mm
eGFP
G
1.0 mm
Pgp → eGFP BAC
H
Human
40X
I
Human
60X
BBB
Pgp
J
Mouse
100X
K
Monkey
100X

Fig 2

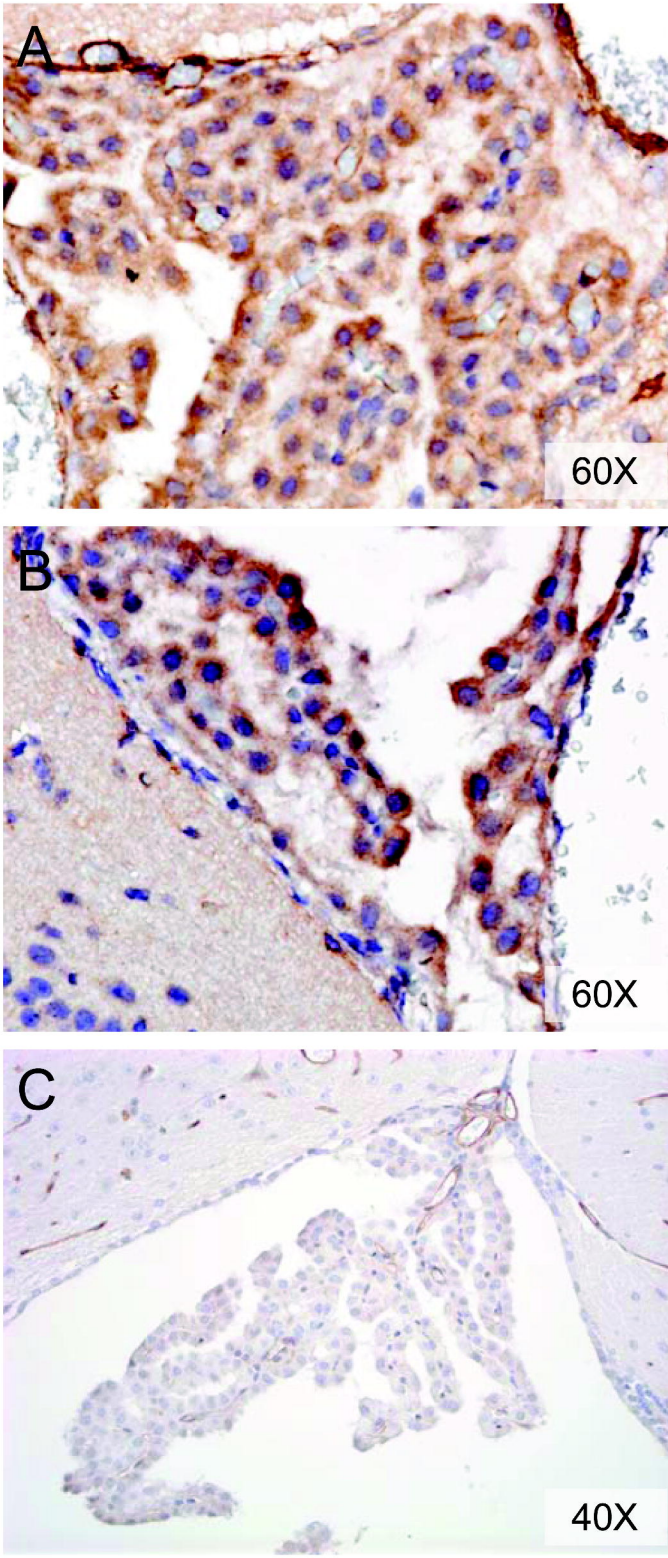

Fig 3

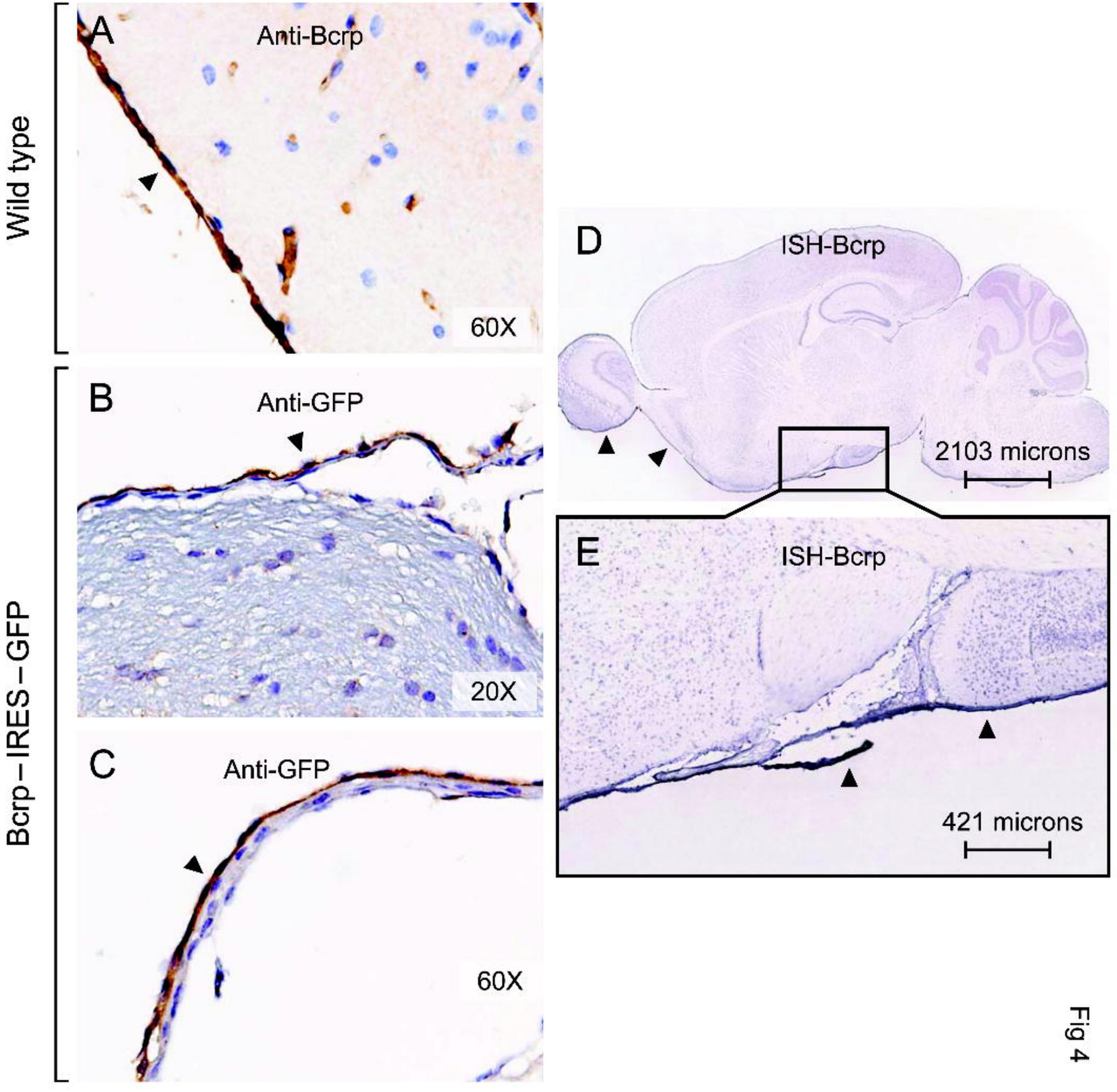
Wild type
A
Anti-Bcrp
60X
Bcrp – IRES – GFP
B
Anti-GFP
20X
C
Anti-GFP
60X
D
ISH-Bcrp
2103 microns
E
ISH-Bcrp
421 microns

Fig 4

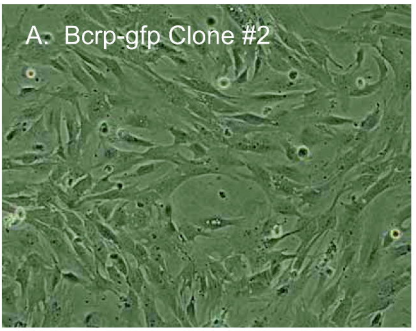
A. Bcrp-gfp Clone #2

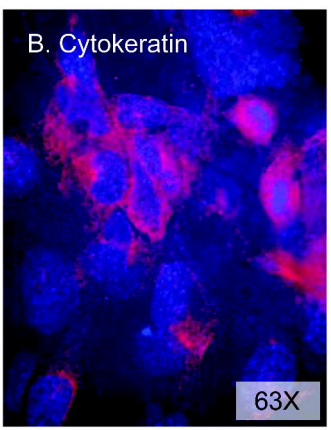
B. Cytokeratin
63X

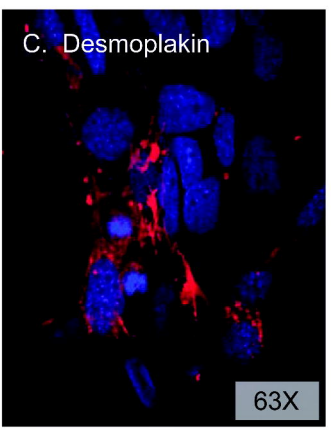
C. Desmoplakin
63X

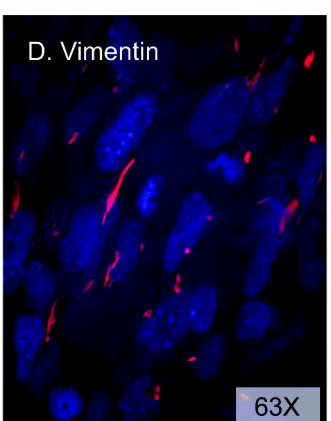
D. Vimentin
63X

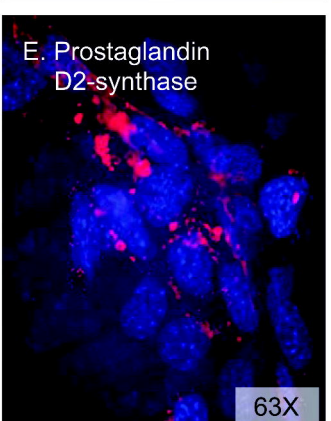
E. Prostaglandin
D2-synthase
63X

Fig 5

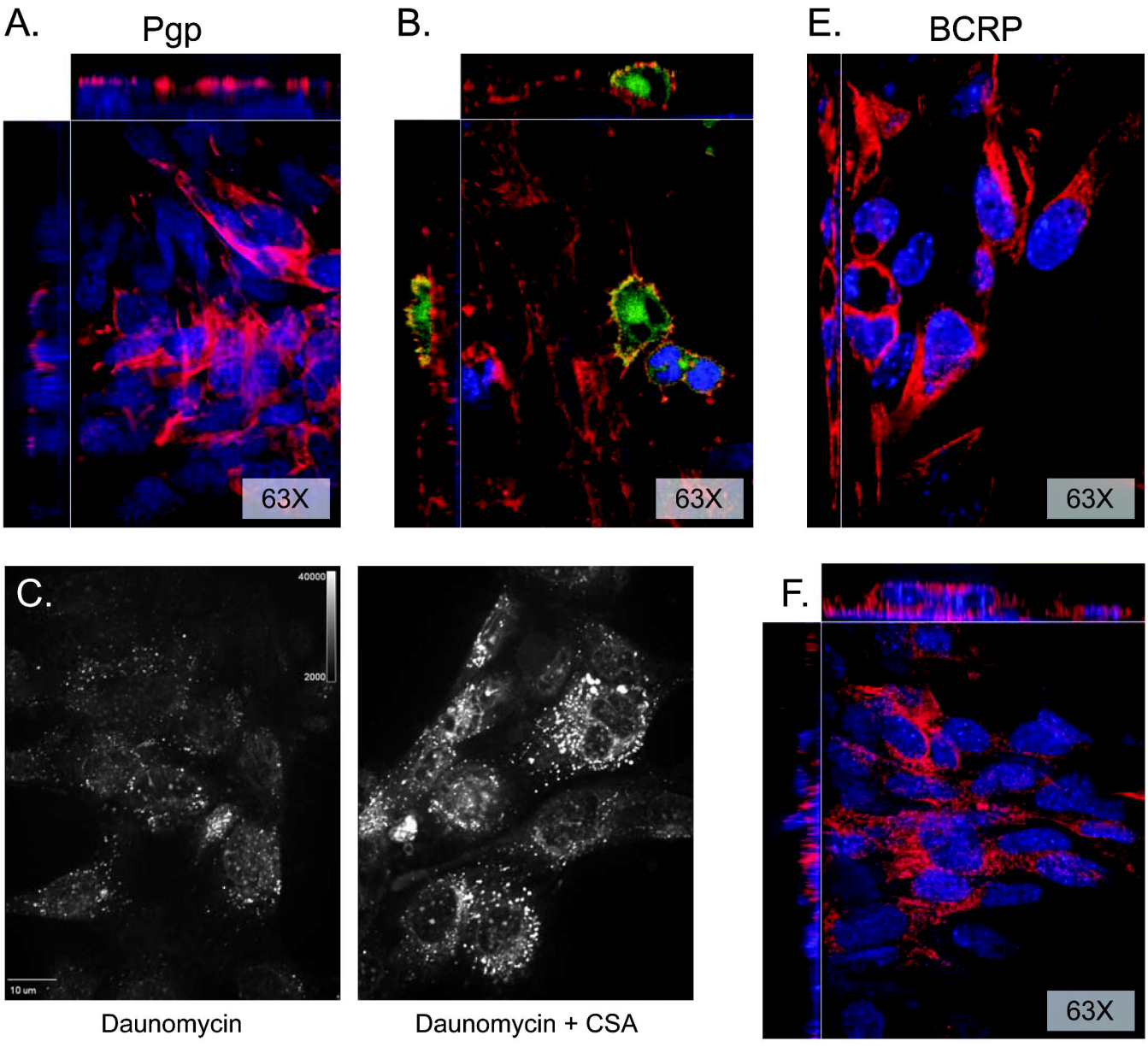
A.
Pgp
63X
B.
63X
E.
BCRP
63X
C.
40000
2000
10 um
Daunomycin
Daunomycin + CSA
F.
63X
D.
Fold Increase over substrate alone
3.0
2.5
2.0
1.5
1.0
0.5
0.0
**
**
Calcein AM + 1μM CsA
Ro800 + 10μM ECD
G.
Fold Increase over mitoxantrone alone
3
2
1
0
**
mitoxantrone
+ FTC

Fig 6